ELSEVIER

Coordination Chemistry Reviews
206–207 (2000) 631–650

COORDINATION CHEMISTRY REVIEWS

www.elsevier.com/locate/ccr

The use of aluminum and gallium hydrides in materials science

Jolin A. Jegier, Wayne L. Gladfelter *

Department of Chemistry, University of Minnesota, Minneapolis, MN 55455, USA

Received 27 October 1999; received in revised form 14 January 2000; accepted 14 January 2000

Contents

---

* Corresponding author. Tel.: + 1-612-6246000; fax: + 1-612-6267541.
E-mail address: gladfelt@chem.umn.edu (W.L. Gladfelter).

PII: S0010-8545(00)00300-3

Abstract

The use of aluminum and gallium hydrides as molecular precursors has been an important development in the field of materials science. Alanes and gallanes have been used in a variety of techniques, such as chemical vapor deposition and solution-based methodologies, to synthesize materials ranging from aluminum thin films to nanocrystalline 13–15 materials. This review is intended to capture the general features of the use of alanes and gallanes in the synthesis of solid state materials.

Keywords: Hydrides; Materials science; Solid state material

1. Introduction

The use of aluminum and gallium hydrides as molecular precursors is a relatively young and developing area of materials science. While compounds such as trimethylamine alane (TMAA), $H_3Al \cdot NMe_3$, have been known for some time [1], it has only been in the last decade or so that these compounds have become the focus of intense fundamental research. The same can be said for applied research involving these compounds; while potential materials science applications appeared in the patent literature in the late 1960s [2–4], the viable use of these compounds as molecular precursors has been explored in depth only recently. The reason for this appears to be 2-fold. First, the lack of fundamental studies involving the group 13 hydrides resulted in a small number of hydride compounds suitable for use as molecular precursors. Secondly, materials applications typically have employed commercially available group 13 alkyls as the source of the group 13 metal. The ever-increasing performance of electronic devices, however, has resulted in increased demands on the physical characteristics of the materials, such as purity, used to construct the devices. This increased demand for purity, as well as the development of novel materials and new materials synthesis techniques, has fueled the renewed interest in the hydrides of group 13. It is the intent of this review to present a broad overview of the emerging use of aluminum and gallium hydride compounds in the synthesis of new or improved materials.

The physical and chemical properties of the group 13 metal hydrides have been reviewed extensively elsewhere [5–8] and will not be detailed here. However, the group 13 hydrides do possess several notable characteristics that make them attractive as precursors to solid state materials. The first feature which makes group 13 hydrides attractive as precursor molecules is the lack of (or in the case of dimethylaluminum hydride, a reduced number of) metal–carbon bonds. The replacement of metal–carbon bonds with metal–hydride bonds in a molecular precursor has the potential to reduce the amount of carbon impurities in the final material. The replacement of metal–carbon bonds in a molecular precursor with thermally frail metal–hydride bonds also has the potential to reduce processing temperatures during the synthesis of the material. This is an important consideration in the construction of fragile electronic devices. A second feature that makes the group 13 hydrides attractive as precursors is the volatility of many hydride derivatives; trimethylamine alane, a solid, has a vapor pressure of 1.23 Torr at 20°C making it approximately 100 times more volatile than liquid $AlEt_3$ [9].

It should be noted that space limitations have prevented the citation of every publication dealing with the use of aluminum and gallium hydrides as molecular precursors. This goal of this review is to capture the general features of the use of alanes and gallanes in materials science; it is not intended to be comprehensive. It should also be noted that quantitative comparisons of results obtained in different laboratories are difficult, at best, and often meaningless. More helpful are those studies in which a comparison of two or more precursors highlights the differences obtained under similar conditions.

2. Metals

2.1. Metal thin films

Thin films of aluminum have seen more wide spread application than the other group 13 metals. A major use of aluminum thin films, owing to the low resistivity of Al°, is as interconnects in microelectronic devices. Another technologically important use of Al° thin films involves the metallization of polymers. Aluminum coated polypropylene has been used as a gas diffusion barrier and, due to the high reflectivity of Al°, aluminum coated polycarbonate is used in compact disks. Alanes, as a class of compounds, are ideal precursors to Al° due to their clean, low temperature decomposition pathway (Eq. (1)). As mentioned previously, while this fact was noted in the late 1960s [2–4], it is only recently that the alanes have been used for metallization purposes.

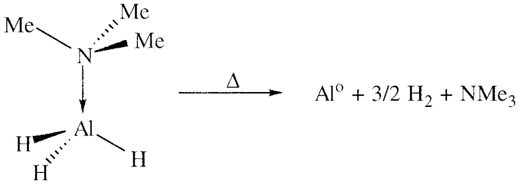

(1)

2.1.1. Al thin films

The chemical vapor deposition of aluminum films has been reviewed previously [10], and only recent developments will be discussed. The two most widely studied aluminum hydride precursors for the chemical vapor deposition of aluminum are dimethylaluminum hydride (DMAH), Me_2AlH [11–26] and dimethylethylamine alane (DMEAA), $H_3Al \cdot NMe_2Et$ [10,27–42]. Other precursors which have been investigated include trimethylamine alane (TMAA), $H_3Al \cdot NMe_3$ [43–45], bis(trimethylamine) alane, $H_3Al \cdot 2\ NMe_3$ [46], triethylamine alane (TEAA), $H_3Al \cdot NEt_3$ [47], tetramethylethylenediamine alane (TMEDAA), $H_3Al \cdot (Me_2NCH_2)_2$ [48], *N*,*N*-dimethyl-*N′*-ethylethylenediamidoalane (DMEEDA), $H_2Al\{N(Et)C_2H_4NMe_2\}$ [49], and the dimethylethylamine adduct of dimethylaluminum hydride, $Me_2AlH \cdot NMe_2Et$ [50]. The structures of these precursors are depicted in Fig. 1.

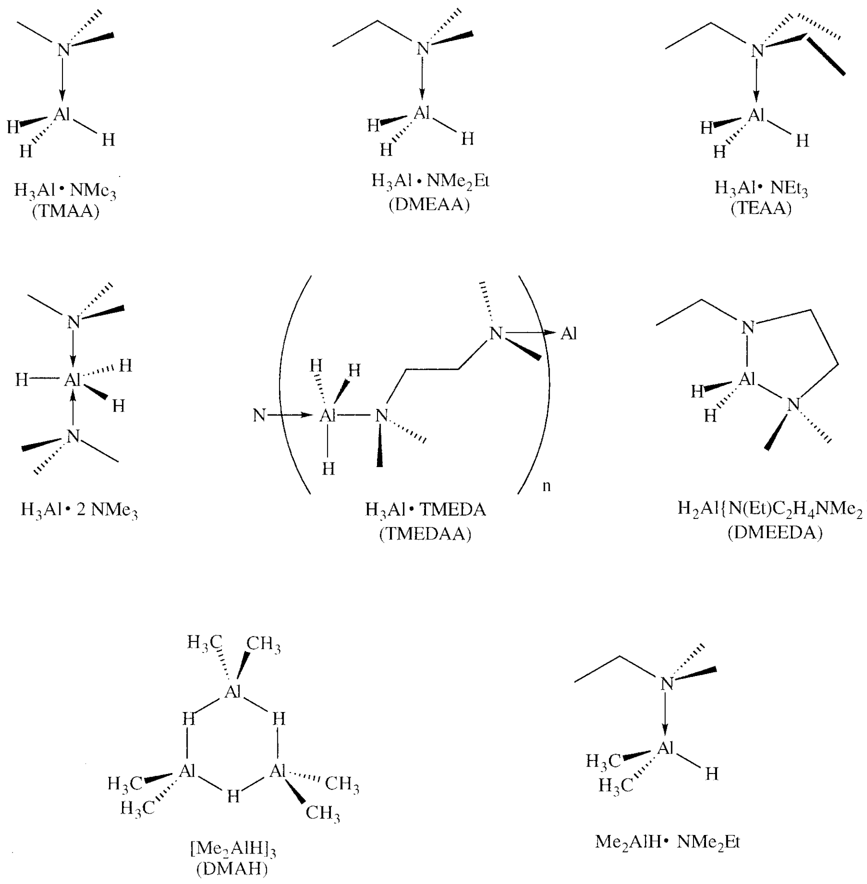

$H_3Al \cdot NMe_3$ (TMAA)

$H_3Al \cdot NMe_2Et$ (DMEAA)

$H_3Al \cdot NEt_3$ (TEAA)

$H_3Al \cdot 2\ NMe_3$

$H_3Al \cdot TMEDA$ (TMEDAA)

$H_2Al\{N(Et)C_2H_4NMe_2\}$ (DMEEDA)

$[Me_2AlH]_3$ (DMAH)

$Me_2AlH \cdot NMe_2Et$

Fig. 1. Aluminum hydrides used as precursors to aluminum-containing thin films.

Since its first use in the late 1960s, $H_3Al \cdot NMe_3$ has continued to be a precursor of practical and theoretical importance. Trimethylamine alane has most recently been used in laser initiated chemical vapor deposition (LCVD) processes that are being developed as low temperature methods for the direct writing of metal thin films. Thin films of aluminum were grown at room temperature on a variety of substrates including PTFE, silicon and GaAs by irradiation with argon (514 nm) and pulsed nitrogen (337 nm) lasers [44]. It was found that this process resulted in little or no laser damage to the substrate, making it a viable method for the construction of delicate microelectronic devices. These methods can be used to make patterned depositions with 1 μm resolution. Aluminum dots have also been deposited using an LCVD process [43]. A 45 μm diameter Ar laser was used to heat a SiO_2/Si substrate from the back (SiO_2) side resulting in the growth of Al dots on the front (Si) side. The size (height and diameter) and shape of the dots could be controlled by varying parameters such as the laser power and deposition time. The dots were typically 20–40 μm in diameter and nearly 1 μm in height. Trimethylamine alane, owing to its well understood reaction chemistry, has also been used to study the interactions of alane precursors with metal oxide surfaces such as SiO_2 [45].

Several alternative alane precursors have also been studied. Triethylamine alane was developed as a liquid alternative to $H_3Al \cdot NMe_3$ [47]; liquid CVD precursors typically exhibit more reproducible vapor pressures and deposition rates making them more amenable to large-scale industrial processes. It was found that the rate determining step in the decomposition of $H_3Al \cdot NEt_3$ to Al° involved desorption of H_2 from the substrate rather than dissociation of the Al-donor bond as in $H_3Al \cdot NMe_3$. This was attributed to the slightly weaker Al–N bond in $H_3Al \cdot NEt_3$. Two other precursors, $H_2Al\{N(Et)C_2H_4NMe_2\}$ [49] and $H_3Al \cdot (Me_2NCH_2)_2$ [48] have been examined as thermally stable alternatives to precursors such as Me_2AlH and $H_3Al \cdot NMe_2Et$. Both compounds were found to be stable at temperatures in excess of 100°C. However, $H_2Al\{N(Et)C_2H_4NMe_2\}$ seemed to be a more viable precursor in that it is a volatile liquid as opposed to a polymeric solid and produces films with a much smoother surface morphology. The smoothness of the films was attributed to a surface-only decomposition pathway; no particle formation due to gas phase reactions was observed. The decomposition temperature was also found to be substrate dependent. Dimethylethylamine alane was also developed as an alternative to $H_3Al \cdot NMe_3$ and $H_3Al \cdot NEt_3$ [28]. Like $H_3Al \cdot NEt_3$, $H_3Al \cdot NMe_2Et$ is a liquid with a high vapor pressure. Dimethylethylamine alane appears to be more thermally stable than $H_3Al \cdot NEt_3$, which decomposes at temperatures above 40°C. Like other alane derivatives, $H_3Al \cdot NMe_2Et$ tends to decompose over time at ambient conditions making long term storage a potential problem. Dimethylethylamine alane also undergoes a small amount of dissociation of the Al–N bond during distillation producing $[AlH_3]_\infty$ and free NMe_2Et, which can lead to inconsistent vapor pressures.

Dimethylethylamine alane, however, has proven to be an excellent precursor for the deposition of aluminum thin films by a variety of methods including metalorganic chemical vapor deposition (MOCVD) [14,27,29–33,35,36,38,42], LCVD

[34,39], and metalorganic molecular beam epitaxy (MOMBE) techniques [37,41]. Thin Al films can be produced from $H_3Al \cdot NMe_2Et$ at temperatures ranging from 100 to 700°C using these techniques. Aluminum deposition using $H_3Al \cdot NMe_2Et$ as the precursor was also found to be extremely substrate dependent. Growth activation energies were lower and growth rates were higher for TiN than they were for SiO_2 [32]. This difference was attributed to differences in the conductivity of the substrate. These substrate effects were utilized in the selective area growth of Al [30]. At low temperatures (100°C) Al was selectively deposited on Au over SiO_2. This selectivity was also utilized in an LCVD two-step writing process that involved the formation of laser nucleated lines followed by a selective area deposition of aluminum on the nucleated pattern [34]. The formation of particles due to gas phase decomposition and reactions during the MOCVD process was also studied using $H_3Al \cdot NMe_2Et$ as the molecular precursor [29]. The formation of these particles was attributed to the presence of trace impurities admitted during the MOCVD process. Heteroepitaxial Al films have also been grown via MOMBE using $H_3Al \cdot NMe_2Et$ [37,41].

A comparison of the microstructure of the Al films deposited on GaAs(100) 2×4 substrates by CVD and evaporative methods has also been described [51]. The films deposited by CVD using $H_3Al \cdot NMe_2Et$ at low temperatures (100–160°C) exhibited a dominant (111) texture that was not evident in the evaporated films. These results suggested that at low enough deposition temperatures, the specifics of the CVD process affect the film microstructure. At these lower temperatures, the growth rate was limited by the surface reaction rate of the impinging precursor molecules resulting in a reduction in the surface mobility of the Al atoms on the surface. This reduction in surface diffusion likely caused the observed difference in texture. At elevated temperatures, the growth rate is in the flux limited regime and the morphologies of the films produced via CVD and evaporation are nearly identical.

Dimethylaluminum hydride is another liquid precursor possessing a high vapor pressure (2 Torr at 20°C) which has been used to deposit high quality aluminum thin films. Deposition of Al° under MOCVD conditions using Me_2AlH typically requires higher temperatures than when alane precursors are employed (200°C for Me_2AlH vs. 100°C for typical alane precursors). The physical properties of the aluminum thin films produced from Me_2AlH were found to be temperature dependent; C incorporation and film resistivity increased with increasing reaction temperatures [22]. This was attributed to the formation of Me_3Al at temperatures above 220°C. Dimethylaluminum hydride was used to deposit Al on Ti, TiO_2, and Pd substrates using photochemical vapor deposition [26]. Growth rates were greatest on Ti (0.5 nm min^{-1} at 60°C) while UV light inhibited the growth of Al on Pd resulting in the thermal deposition of Al. Like $H_3Al \cdot NMe_2Et$, dimethylaluminum hydride has been used as the precursor in the selective area growth of Al [11,13]. Aluminum CVD using Me_2AlH is also being explored as an alternative to tungsten plug technology [21].

The initial stages of Al thin film growth from Me_2AlH has been studied in great detail using a variety of techniques such as IR [12,25] and X-ray photoelectron [23] spectroscopies and scanning tunneling microscopy [17,20]. At room temperature the

Me_2AlH molecules were adsorbed intact, presumably as dimers, on the surface. At 350 K, the decomposition was observed to occur on the surface to form Al dimer rows as the initial stage of nucleation. Above 400 K, the dissociation of Me_2AlH occurs before the molecules interact with the surface and it was found that the best films of Al were deposited above this temperature [20].

However, there are some drawbacks to the use of Me_2AlH. Firstly, in the gas phase it exists as the trimer, but in the condensed phase it is a highly viscous, presumably polymeric, liquid (6400 cP) [14,16]. This viscosity hinders its vaporization in the precursor bubblers typically used in MOCVD. Secondly, Me_2AlH is extremely pyrophoric, making it somewhat dangerous to store and use. A couple of approaches have been taken to combat these problems. The addition of additives such as *N*-ethyl-*N*-methylaniline, *N*,*N*-dimethyl-1-naphthylamine, tribenzylphosphine or trihexylamine can reduce the viscosity of Me_2AlH from 6400 to 6–60 cP at concentrations as low as 3 mol% [14,16]. The reaction of Me_2AlH with NMe_2Et to form the adduct $Me_2AlH \cdot NMe_2Et$ resulted in a precursor that was a non-pyrophoric, free flowing liquid that produced good quality Al films in a cold-walled quartz reactor [50].

2.2. Nanocrystalline metals

There has also been a growing interest in the synthesis of nanocrystalline metals, such as Al and its intermetallics, owing to the improved mechanical properties exhibited by these materials. These properties include increased strength, hardness, ductility and toughness. Nanocrystalline metal powders are also typically more reactive than bulk metals, making them attractive as precursors to quantum dots of electronic materials. Nanoscale aluminum powders are also of interest for propellant, explosive and powder metallurgical applications. Nanocrystalline intermetallics, such as titanium aluminide, are valued for their low densities and high temperature strengths. The use of aluminum hydride precursors has led to the development of low temperature routes to extremely pure and reactive nanocrystalline metals as well as a variety of intermetallics.

2.2.1. Nanocrystalline Al

Two different chemical routes have been used to synthesize nanocrystalline Al. The first method involved the reaction of lithium aluminum hydride, $LiAlH_4$, and $AlCl_3$ in 1,3,5-trimethylbenzene at 164°C, while the second involved the thermal decomposition of $H_3Al \cdot NMe_2Et$ in 1,3,5-trimethylbenzene at 164°C in the presence of varying amounts of a titanium isopropoxide catalyst (Eqs. (2) and (3)) [52]. The thermal decomposition of $H_3Al \cdot NMe_2Et$ was found to lead to better control over product coherence length with particle sizes ranging from 44 to 197 nm depending upon catalyst concentration, as well as to nanocrystalline aluminum powders of greater purity. The nanocrystalline aluminum powders synthesized in this study were also found to undergo facile grain growth, which was attributed to their chemical purity.

$$3LiAlH_4 + AlCl_3 \rightarrow 4\ \text{nano-Al} + 3LiCl + 6H_2 \qquad (2)$$

$$H_3Al \cdot NMe_2Et \rightarrow \text{nano-Al} + 3/2H_2 + HMe_2Et \qquad (3)$$

Nanocrystalline aluminum was also synthesized via the thermolysis of $H_3Al \cdot NMe_3$ in the presence of TMEDA and titanium isopropoxide in toluene or xylene solvent at temperatures ranging from 50 to 140°C [53]. The aluminum powders isolated from these reactions ranged in size from < 100 to 500 nm as estimated by SEM. The particles, after passivation with O_2 to produce a surface oxide layer, contained from 61 to 92% Al depending upon crystallite size. The quality of the nanocrystalline Al was similar to that produced from other methods such as aluminum vapor condensation and exploded Al wire techniques.

2.2.2. Nanocrystalline Al intermetallics

Aluminum containing intermetallics such as titanium and nickel aluminides have also been synthesized by chemical means using aluminum hydride derivatives. The titanium aluminide, $TiAl_3$ was synthesized by the reaction of tris(bis(trimethylsilyl)amido)titanium (III), $Ti[N(SiMe_3)_2]_3$, and AlH_3 in hexane/diethyl ether solution (Eq. (4)) [54]. The resulting solid was then heated to 1000°C to produce $TiAl_3$ that was contaminated with small amounts of TiO and Ti_3Al. The product also contained significant amounts of C, H and O. The $TiAl_3$ particles were found to range in size from 5 to 25 nm.

$$Ti[N(SiMe_3)_2]_3 + AlH_3 \rightarrow \text{Ti/Al precursor} \xrightarrow{1000°C} TiAl_3 \qquad (4)$$

$TiAl_3$, as well as TiAl, NiAl and Ni_3Al were also synthesized via the reaction of $LiAlH_4$ with the appropriate amount of either $TiCl_3$ or $NiCl_2$.[55] The overall reactions can be seen in Eqs. (5)–(8). These reactions resulted in the formation of precipitates that were converted to the desired materials at temperatures ranging from 550 to 750°C. The reaction chemistry was found to involve the formation of unidentified reduced Ni and Ti species and nanocrystalline Al in the initial precipitate, which then reacted to form intermediate phases such as Ni_2Al_3 and Ti_2Al_5 during heating. The TiAl, $TiAl_3$, NiAl and Ni_3Al crystallite diameters ranged from 25 to 41 nm. The coherence length of these samples was believed to be determined during the initial reaction between the reduced metals, rather than during the annealing stage.

$$2TiCl_3 + 3LiAlH_4 \rightarrow 2TiAl + AlCl_3 + 3LiCl + 6H_2 \qquad (5)$$

$$TiCl_3 + 3LiAlH_4 \rightarrow TiAl_3 + 3LiCl + 6H_2 \qquad (6)$$

$$4NiCl_2 + 5LiAlH_4 \rightarrow 4NiAl + AlCl_3 + 5LiCl + 10H_2 \qquad (7)$$

$$12NiCl_2 + 9LiAlH_4 \rightarrow 4Ni_3Al + 5AlCl_3 + 9LiCl + 12H_2 \qquad (8)$$

3. 13–15 Materials

3.1. Thin films of 13–15 materials

Due to their wide range of band gaps and ability to form solid solutions, thin films of 13–15 semiconductor materials and their alloys are technologically important electronic materials. Materials such as AlGaAs and AlGaN are being used in optoelectronic devices. As was the case for the deposition of Al°, there has been recent interest in developing new group 13 precursors to increase the performance of devices based on these 13–15 materials.

3.1.1. Al Containing 13–15 films

The development of alanes as alternative Al precursors to 13–15 thin films continues to be an area of intense research. This research has been driven by the fact that, while good quality films and devices have been manufactured with precursors such as aluminum alkyls, the use of aluminum alkyls leads to substantial carbon and oxygen incorporation. The carbon incorporation is due to the presence of the relatively strong Al–C bonds in the precursor [56], while the oxygen incorporation is proposed to be due to aluminum alkoxide impurities which are often present in aluminum alkyls [57]. The use of alane derivative precursors is expected to reduce both C and O incorporation in the final films.

3.1.1.1. AlAs. A number of aluminum hydride precursors, including $H_3Al \cdot NMe_3$ [58–62], $H_3Al \cdot NMe_2Et$ [61,63–73], Me_2AlH [74,75] and the trimethylamine adduct of diethylaluminum hydride ($Et_2AlH \cdot NMe_3$) [68,76], have been used as the aluminum source in the depositions of AlAs and AlGaAs thin films. These precursors have been used in a variety of techniques such as MOCVD, LP-MOVPE, MBE and ALE and led to substantial decreases in impurities, such as C and O.

Several researchers have compared the use of alane precursors with traditional aluminum sources or with other alane precursors. In the MOMBE growth of AlGaAs, $H_3Al \cdot NMe_3$ generally led to higher growth rates, lower carbon and oxygen concentrations and higher crystallinity than did triethylaluminum [60]. While carbon concentrations were generally reduced by an order of magnitude, the use of $H_3Al \cdot NMe_3$ resulted in a lowering of the oxygen concentration by over two orders of magnitude. This reduction supported the hypothesis that the aluminum alkoxides, present in aluminum alkyls, are the main source of oxygen contamination in AlAs deposited by MOMBE. A comparison of AlAs and AlGaAs films grown by MOMBE using $H_3Al \cdot NMe_3$ and $H_3Al \cdot NMe_2Et$ has also been studied. It was found that, in terms of carbon and oxygen contamination, $H_3Al \cdot NMe_2Et$ was a better precursor than $H_3Al \cdot NMe_3$. This was attributed to contamination of the $H_3Al \cdot NMe_3$ by the ethereal solvents used during its synthesis; $H_3Al \cdot NMe_2Et$ can be synthesized in hydrocarbon solvents. While $H_3Al \cdot NMe_2Et$ is also attractive because it is a liquid and yields more reproducible depositions, its lower thermal stability has lead to storage problems.

Dialkylaluminum hydrides have also been used to produce AlGaAs and AlAs thin films. Dimethylaluminum hydride was found to produce AlGaAs films via MOCVD with a lower C content than those produced under similar conditions using trimethylaluminum [74]. Dimethylaluminum hydride was also used in the selective area MOMBE deposition of AlAs films [75]. Using Me_2AlH in combination with tris(dimethylamido)arsine produced smoother and purer films than those produced using a traditional As sources, such as As_4. This selective area growth was not achieved when an alane precursor, such as dimethylethylamine alane was employed [72]. The use of the trimethylamine adduct of diethylaluminum hydride ($Et_2AlH \cdot NMe_3$) led to the growth very pure AlGaAs films by CBE with C and O levels that were below the detection limits (10^{15} and 10^{16} cm^{-3}, respectively) as determined by SIMS [68]. This was accomplished using the traditional Ga and As sources triethylgallium and arsine. The optical and electrical properties of the AlGaAs grown using $Et_2AlH \cdot NMe_3$ were comparable to films grown using other techniques such as MBE.

3.1.1.2. AlSb. Both trimethylamine alane and dimethylethylamine alane have been used in the growth of AlSb and AlSbAs thin films [77–79]. The AlSb layer of (Al,Ga)Sb/InAs resonant interband tunneling diodes was grown by molecular beam epitaxy using $H_3Al \cdot NMe_3$ or Al° as the aluminum source [79]. The use of $H_3Al \cdot NMe_3$ led to the construction of devices with performance characteristics that were comparable to those made using Al°, the typical aluminum source used in MBE. Trimethylamine alane was also used to grow AlSb and $AlAs_xSb_{1-x}$ by MOCVD [77] at 500 and 600°C, respectively using triethylantimony and AsH_3 as the Sb and As sources. The use of $H_3Al \cdot NMe_3$, instead of a traditional aluminum source such as trimethylaluminum, $AlMe_3$, resulted in low C and O incorporation (2×10^{18} and 6×10^{18} cm^{-3}). Because of these low levels of C and O, the first n-type AlSb and AlAsSb alloys were made after doping with tetraethyltin. In the construction of two color LEDs based upon doped Al(As)Sb thin films, liquid dimethylethylamine alane was found to have a more consistent vapor pressure than solid trimethylamine alane, resulting in more reproducible depositions [78].

3.1.1.3. AlP. Dimethylethylamine alane was found to be an effective aluminum source for the metal–organic chemical vapor deposition of p-type AlGaInP, which is used as the cladding layer material in visible region lasers [80]. Both $AlMe_3$ and $H_3Al \cdot NMe_2Et$ were used as the aluminum source to produce films of $(Al_xGa_{1-x})_{0.5}In_{0.5}P$ ($x = 0.4$ and 0.7) at temperatures of 640 and 720°C using PH_3. It was found that the use of dimethylethylamine alane led to greater hole concentrations and a corresponding higher electrical activity. It was suggested that the observed increase in electrical activity was due to a decrease in oxygen contamination, and that this decreased contamination was a result of using $H_3Al \cdot NMe_2Et$ as the aluminum source.

3.1.1.4. AlN. One of the first attempts to deposit AlN thin films using a hydride precursor involved the thermolysis of bis(dialkylamido)aluminum hydrides,

$[HAl(NR_2)_2]_2$ (R = Me, Et) [81]. Deposition on glass substrates between 300 and 500°C produced amorphous films. After annealing at 1300°C, the films displayed X-ray diffraction patterns consistent with AlN. Since this initial attempt, thin films of AlN have been grown via CVD and MBE techniques using $H_3Al \cdot NMe_3$ [9,82–84]and $H_3Al \cdot NMe_2Et$ [85–90] as the aluminum precursors.

Trimethylamine alane was used as an aluminum precursor in the low-pressure (76 Torr) metalorganic chemical vapor deposition of AlN and AlGaN thin films at 1050°C using NH_3 as the nitrogen source [9,83]. Under these conditions, the C and O incorporation was nearly identical (10^{17} and 10^{21} cm^{-3}, respectively) to that obtained when $AlEt_3$ was used as a precursor. However, it was found that the use of $H_3Al \cdot NMe_3$ led to growth rates ten times greater than those obtained from $AlEt_3$, and that these films exhibited improved optical and crystalline properties. As was the case for AlAs, the use of $H_3Al \cdot NMe_2Et$ in the CBE growth of AlN led to films with lower C and O incorporation than those grown using $H_3Al \cdot NMe_3$ [89].

Trimethylamine alane and NH_3 have also been used to grow AlN at temperatures from 380 to 675 K via an atomic layer growth process [82,84]. Repeated, alternated exposure of a surface to NH_3 and $H_3Al \cdot NMe_3$ led to the growth of high quality AlN thin films. This atomic layer growth proceeded by adsorption of the $H_3Al \cdot NMe_3$ onto the surface followed by the displacement of the NMe_3 by NH_3, and subsequent elimination of H_2 to form Al–NH_2 species on the surface. Repeated exposure to $H_3Al \cdot NMe_3$ and NH_3 resulted in reaction with the surface NH_2 groups to form AlN via loss of H_2, and the generation of a new Al–NH_2 surface. Similar results were obtained using $H_3Al \cdot NMe_2Et$ as the aluminum source.

3.1.2. Ga containing 13–15 films

Gallane derivatives have also been used in the growth of 13–15 thin films, albeit to a much lesser extent than the alanes. The use of gallanes as CVD and MBE precursors has been hindered by the thermal instability of many gallane derivatives and the involatility of those derivatives that are more thermally stable [91]. The current 'state of the art' Ga sources for the production of Ga containing 15–15 films by processes such as CVD, CBE and MBE continue to be trialkylgallium species such as trimethyl- and triethylgallium. The use of alternative Ga sources such as triisobutylgallium have not produced the dramatic improvement in film purity observed for the use of alternative Al sources such as alane derivatives [91]. Several reported examples of the use of gallane as alternative Ga sources, however, have indicated that properly designed gallium hydride compounds can be effective precursors to thin films of Ga containing 13–15 materials Fig. 2.

3.1.2.1. GaAs. Quinuclidine–gallane was found to be sufficiently stable and volatile at 60°C to be used as the gallium source in the growth of GaAs by MOMBE, and showed significant advantages over the thermally frail $H_3Ga \cdot NMe_3$ and involatile $H_3Ga \cdot DMPE$ and $H_3Ga \cdot TMEDA$ (DMPE = $(Me_2PCH_2)_2$; TMEDA = $(Me_2NCH_2)_2$) [91]. Growth experiments, using As_4 as the As source, were carried out at temperatures ranging from 300 to 800 K. The maximum growth rate was observed at 450 K, which was much lower temperature that that of observed for

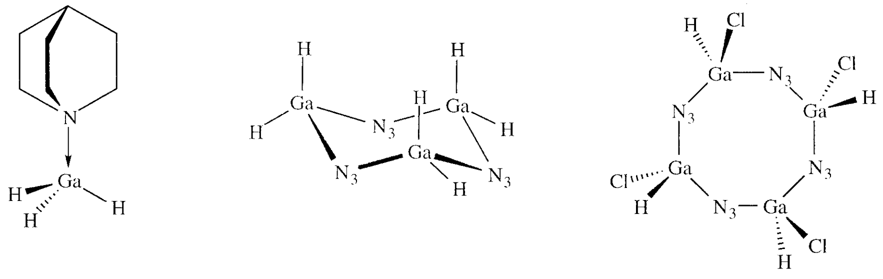

$H_3Ga \cdot$ quin $[H_2GaN_3]_3$ $[H(Cl)GaN_3]_4$

Fig. 2. Gallane precursors used as precursors to thin films of 13–15 thin films.

other Ga sources such as trialkyl gallium compounds. Associated thermal desorption studies indicated that $H_3Ga \cdot$quinuclidine was a viable, low carbon Ga precursor for use in the MBE growth of 13–15 materials and possessed adsorption and decomposition pathways similar to that of the alane derivatives.

3.1.2.2. GaN. The 'single-source precursor' approach to materials has also been examined using gallane derivatives. The hydridogallium azide, $[H_2GaN_3]_n$ was synthesized from $[H_2GaCl]_2$ and LiN_3 and was found to be an effective precursor to GaN thin films [92–94]. Stoichiometric GaN which was free of C, N and O was grown under UHV–CVD conditions between 150 and 800°C. The only observed byproducts observed during growth were H_2 and N_2, making this a very clean precursor. Growth on Si at 200°C and 10^{-4} Torr, produced films composed of nanometer sized crystallites, while heteroepitaxial growth of GaN was achieved at 650°C and 2×10^{-6} Torr on sapphire substrates. The high reactivity and sensitivity of $[H_2GaN_3]_n$, however, makes it unlikely that it will become a practical precursor to GaN films. The related, tetrameric, azidochlorogallane $[Cl(H)GaN_3]_4$ was also found to be sufficiently volatile and produced stoichiometric GaN films on sapphire substrates between 500 and 600°C [93]. The films deposited at 600°C were found to be free of chlorine impurities.

3.2. Nanocrystalline 13–15 materials

The synthesis of nanocrystalline 13–15 compounds such as GaAs, GaN and InP has also been a subject of intense research due to the size, or quantum confinement, effects exhibited by these materials [95]. For example, the observation that the bandgaps of these materials increase with decreasing particle size has driven researchers to develop new chemical methods for the syntheses of these materials with the goal of controlling particle purity, particle size and particle size distribution. The relative frailty of the Al–H and Ga–H (compared to Al–C and Ga–C) moieties has made alane and gallane derivatives especially attractive for the low temperature syntheses of these materials.

3.2.1. AlN

Several approaches have been taken in the synthesis of micro- and nanocrystalline AlN and AlN composites. The reaction of $LiAlH_4$ with NH_4X ($X = Cl$, Br) resulted in the polymeric hydridoaluminum imide, $[HAlNH]_n$ (Eq. (9)) [96]. This precursor was pyrolyzed at temperatures ranging from 200 to 950°C under N_2, NH_3, and dynamic vacuum. Complete conversion to microcrystalline AlN occurred at 950°C. The reactions of $[HAlNH]_n$ with hydrazine, N_2H_4, and of $LiAlH_4$ with hydrazine hydrochloride, $N_2H_4 \cdot HCl$, also resulted in alane precursors that produced good quality (< 0.5% carbon) microcrystalline AlN powders.

$$\mathrm{LiAlH_4 + NH_4Br} \xrightarrow[\substack{-\,\mathrm{LiBr}\\ -\,3\,\mathrm{H_2}}]{} 1/\mathrm{n}\,[\mathrm{HAlNH}]_\mathrm{n} \xrightarrow[-\,\mathrm{n\,H_2}]{950\,^{\circ}\mathrm{C}} \mathrm{AlN} \tag{9}$$

A second approach to nanocrystalline AlN involves the direct nitridation of nanocrystalline Al° at 1000–1100°C [97]. The nanocrystalline Al° powders were produced as described above via the reduction of $H_3Al \cdot NMe_2Et$ in the presence of a titanium isopropoxide catalyst (Eq. (10)). The high reactivity of the nanocrystalline Al° produced from this reduction allowed for direct nitridation to form either equiaxed AlN nanocrystals (25–50 nm) or AlN nanowhiskers. The nanowhiskers were produced in the presence of $AlCl_3$ via a vapor–solid (VS) mechanism and typically had a diameter of 20–100 nm.

$$\mathrm{H_3Al \cdot NMe_2Et} \xrightarrow[\mathrm{Ti(O^{\mathit{i}}Pr)_4}]{164^{\circ}\mathrm{C}} \text{nano Al} \xrightarrow[\mathrm{AlCl_3}]{1000^{\circ}\mathrm{C}} \text{AlN nanowhiskers} \tag{10}$$

AlN/BN nanocrystalline composites have also been synthesized via the reaction of $H_3Al \cdot NMe_3$ and ammonia borane, $H_3B \cdot NH_3$ (Eq. (11)) [98]. The reaction of $H_3Al \cdot NMe_3$ and $H_3B \cdot NH_3$ in toluene (in 1:1 and 1:2 molar ratios) followed by reaction with NH_3 resulted in the elimination of NMe_3 and H_2 and the isolation of ceramic precursors containing Al–N–B linkages. These precursors were pyrolyzed at 1000°C under NH_3, which resulted in the formation of nanoscale AlN/BN composite particles composed of crystalline AlN and amorphous BN.

$$\mathrm{H_3Al{\bullet}NMe_3 + H_3B{\bullet}NH_3} \xrightarrow{\substack{\text{1) toluene}\\ \text{2) NH}_3}} \text{Al-N-B precursor} \xrightarrow{1000\,^{\circ}\mathrm{C}} \text{AlN/BN composite} \tag{11}$$

3.2.2. GaN

Gallium hydride derivatives have been used extensively in the synthesis of nanocrystalline GaN, which represents one of the most studied nanocrystalline 13–15 materials. The first reported synthesis of nanocrystalline GaN involved the pyrolysis of cyclotrigallazane, $[H_2GaNH_2]_3$, which had been synthesized from $H_3Ga \cdot NMe_3$ and NH_3 (Scheme 1) [99]. Pyrolysis of $[H_2GaNH_2]_3$ at 600°C resulted in the formation of a gallium rich ($GaN_{0.83}$) material which was found to be a mixture of cubic and hexagonal GaN, and had an average coherence length of 6 nm. Computer modeling of the X-ray intensity data suggested that the nanocrystals

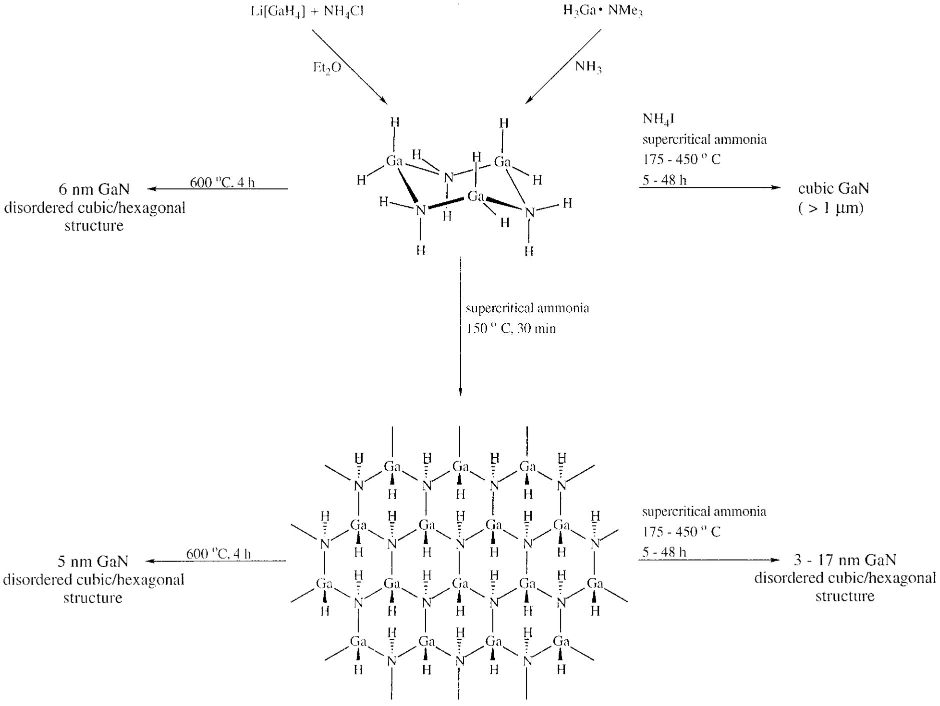

Scheme 1.

possessed a disordered structure containing a random arrangement of cubic and hexagonal close packed layers rather than a simple physical mixture of the cubic and hexagonal planes [100]. The formation of the cubic portions of the structure was proposed to be due to a partial topochemical conversion of $[H_2GaNH_2]_3$ to GaN. Analysis of the crystal structure of $[H_2GaNH_2]_3$ revealed that the positions of the Ga and N atoms resembled a significant portion of GaN possessing the zinc blende structure [100,101]. A report detailing an alternative synthesis of $[H_2GaNH_2]_3$, involving the reaction of Li[GaH$_4$] and NH_4Cl, and its thermolysis to form nanocrystalline GaN has also been published [102,103]. The nanocrystalline GaN produced via this alternative synthesis was nearly identical to that produced from $H_3Ga \cdot NMe_3$ and NH_3.

Cyclotrigallazane has also been converted to a polymeric GaN precursor, and to nanocrystalline GaN in supercritical ammonia [104]. Heating a solution of $[H_2GaNH_2]_3$ in NH_3 to 150°C for 30 min resulted in the isolation of poly(imidogallane), $[HGaNH]_n$. Poly(imidogallane) was proposed to have a two dimensional network structure on the basis of IR, EA, XRD, TEM and ED data. The formation of $[HGaNH]_n$ was proposed to be due to an ammonia-assisted dehydrogenation via the elimination of both NH_3 and H_2 [105]. Pyrolysis of $[HGaNH]_n$ under N_2 at 600°C resulted in the isolation of a pale yellow GaN powder which, like the GaN obtained from the pyrolysis of $[H_2GaNH_2]_3$, possessed a disordered structure consisting of a random arrangement of cubic and hexagonal close packed planes. The average coherence length was found to be 5 nm. Cyclotrigallazane could be converted to GaN in supercritical ammonia, through the $[HGaNH]_n$ intermediate, by increasing the reaction time at 150°C. Reaction times of 5 and 24 h led to nanocrystalline GaN with average coherence lengths of 3 and 4 nm, respectively. The coherence length of the nanocrystals could also be controlled by varying the temperature of the thermolysis [106]. Heating solutions of $[H_2GaNH_2]_3$ in supercritical ammonia for 1000 min at 150, 250, 350 and 450°C resulted in nanocrystalline GaN with coherence lengths of 4, 8, 14 and 17 nm, respectively. XRD and TEM data showed that these nanocrystals also possessed a disordered structure.

Cyclotrigallazane has also been used in one of the first bulk syntheses of phase-pure cubic GaN [106]. Thermolysis of a 1:1 mass ratio of $[H_2GaNH_2]_3$ and NH_4I in supercritical ammonia at temperatures between 175 and 260°C resulted in the synthesis of micron sized crystals of cubic GaN. At temperatures greater than 260°C, mixtures of cubic and hexagonal GaN were produced. TEM and electron diffraction data indicated that the mixture of cubic and hexagonal GaN produced under these conditions was a physical mixture of the two phases and was not due to a disordered structure as in the nanocrystals.

Two other gallium hydride derivatives, $[Cl(H)GaN_3]_4$ and $[H_2GaN_3]_n$, were also found to be effective precursors to nanocrystalline GaN [93,94]. $[Cl(H)GaN_3]_4$ decomposes exothermically above 70°C to form GaN through elimination of HCl and N_2. Like the GaN produced from $[H_2GaNH_2]_3$, the GaN nanocrystals obtained from the thermal decomposition of $[Cl(H)GaN_3]_4$ contain a mixture of the cubic and hexagonal phases. The crystallite size of the GaN obtained from $[Cl(H)GaN_3]_4$ was not reported. The related hydridogallium azide, $[H_2GaN_3]_n$, was also found to decompose exothermically to nanocrystalline GaN via the loss of N_2 and H_2 [93]. $[H_2GaN_3]_n$ was extremely reactive at room temperature with decomposition being initiated by simple physical manipulation of the precursor. This decomposition resulted in the formation of nanocrystalline GaN with a fibrous morphology. GaN fibers were typically 15–20 nm in diameter and several microns in length. They consisted primarily of hexagonal GaN; however, regions of disordered and cubic GaN were also observed by TEM. The material could be converted to phase pure hexagonal GaN after annealing at 800°C.

3.2.3. Other 13–15 materials

There are few reports on the use of hydride precursors for the synthesis of 13–15 materials other than AlN and GaN. Two of the materials that have been synthesized using gallane derivatives are GaP and GaAs [107]. The precursors $[H_2GaE(SiMe_3)_2]_3$ ($E = P$, As) were synthesized by the reaction of $H_3Ga \cdot NMe_3$ with $P(SiMe_3)_3$ or $As(SiMe_3)_3$ via a dehydrosilylation reaction (Eq. (12)). These compounds also represented the first examples of phosphino- and arsinogallanes containing hydrido substituents on the gallium centers. Both of these compounds were relatively unstable at room temperature, and underwent further dehydrosilylation (among other) reactions to afford polymeric materials. Pyrolysis of

$[H_2GaP(SiMe_3)_2]_3$ at 450 and 600°C resulted in nanocrystalline GaP with average coherence lengths of 2 and 25 nm, respectively. Pyrolysis of the polymeric decomposition product of $[H_2GaP(SiMe_3)_2]_3$ at 475°C produced 5.1 nm GaP nanocrystals. Owing to its instability under ambient conditions, $[H_2GaAs(SiMe_3)_2]_3$ could not be used directly as a precursor to GaAs. Pyrolysis of the polymeric decomposition product of $[H_2GaAs(SiMe_3)_2]_3$ at 450°C, however, produced GaAs nanocrystals with an average crystallite size of 3–4 nm. The GaP and GaAs produced from these precursors were found to be contaminated with Si and C, and this was postulated to be due to decomposition pathways other than dehydrosilylation.

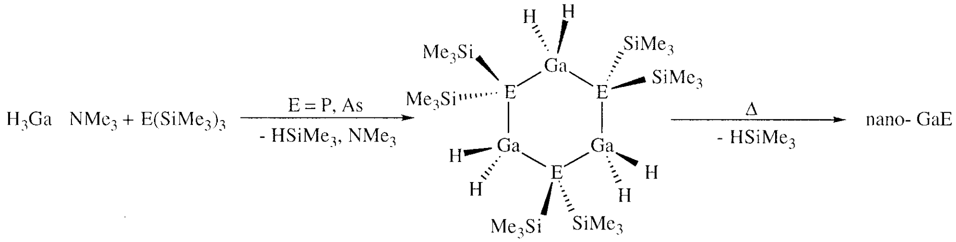

(12)

4. Other materials

4.1. *Group 13–16 materials*

The use of the hydrides of aluminum and gallium for the syntheses of other materials such as 13–16 compounds is considerably less well developed than that of the 13–15 materials. The few reported examples, however, illustrate the potential use of alane and gallane derivatives for the syntheses of other important materials.

4.1.1. *Al_2O_3*

Dimethylethylamine alane has been used for the growth of Al_2O_3 films on Si by MOMBE using O_2 as an oxidant at temperatures ranging from 600 to 900°C [108]. Epitaxial films of Al_2O_3 with low carbon incorporation were grown at 700°C. The use of $H_3Al \cdot NMe_2Et$, rather than $AlMe_3$, as a precursor under these conditions led to a lower epitaxial temperature (700 vs. 800°C) and a decrease in carbon contamination by a factor of five.

Thin films of alumina have also been deposited using a laser assisted chemical vapor deposition (LACVD) method [109]. Laser excitation (4.6 eV) of thin layers of dimethylaluminum hydride and water at 80 K produced pinhole-free films of alumina which were approximately 40 Å thick. Ironically, the use of dimethylaluminum hydride as a precursor led to films with a higher carbon content than those produced using trimethylaluminum as the aluminum precursor.

4.1.2. Al_2S_3

$H_3Al \cdot NMe_3$ was found to react with $S(SiMe_3)_2$ in toluene to form the aluminum sulfide clusters $Al_4S_5(H_2)(NMe_3)_4$ and $Al_4S_6(NMe_3)_4$ via elimination of trimethylsilane (Eq. (13)) [110]. The adamantane-like structure of $Al_4S_6(NMe_3)_4$ represented a solvated form of Al_2S_3. $Al_4S_6(NMe_3)_4$ was converted to amorphous Al_2S_3 under vacuum at approximately 250°C.

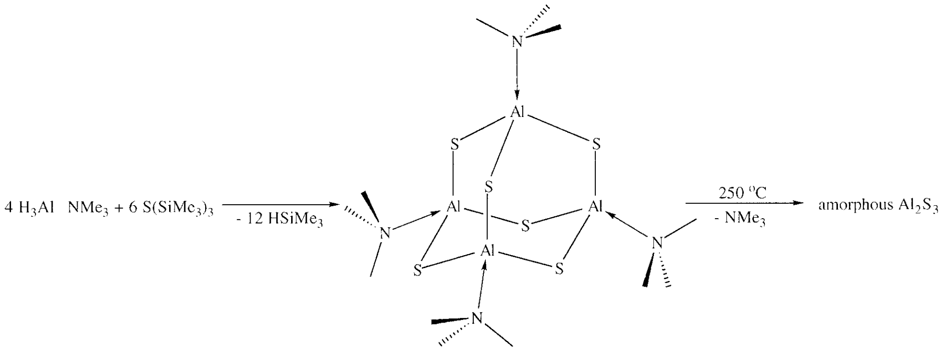

(13)

5. Conclusions

Aluminum and gallium hydride base compounds are an important class of precursors to a variety of solid state materials. The use of these hydrides as precursors has typically lowered processing temperatures and impurity levels and, has led to the development of new synthetic routes to materials. There are trade-offs, however, that must be addressed before these precursors can become economically viable. The thermal frailty of the metal–hydride bond can make long-term storage of these materials problematic. The extreme oxygen and moisture sensitivity of compounds like Me_2AlH can also make handling large quantities of these materials difficult. Current research efforts are aimed at addressing these issues and these efforts should ensure that this class of compounds will continue to be important in the field of materials science well into the future.

Acknowledgements

The authors' research in this area was supported by the National Science Foundation and the Center for Interfacial Engineering at the University of Minnesota. The authors would also like to thank Ms. H.-Y. Park for her assistance in the preparation of this manuscript.

References

[1] E. Wiberg, E. Amberger, Hydrides of the Elements of Main Groups I–!V, Elsevier, Amsterdam, 1971.

[2] T.P. Whaley, V. Norman, US patent, 1965.

[3] D.R. Carley, J.H. Dunn, US patent, 1968.

[4] D.L. Schmidt, R. Hellmann, US patent, 1969.

[5] A.J. Downs, C.R. Pulham, Chem. Soc. Rev. 23 (1994) 175.

[6] C. Jones, G.A. Koutsantonis, C.L. Raston, Polyhedron 12 (1993) 1829.

[7] C.L. Raston, J. Organomet. Chem. 475 (1994) 15.

[8] M.G. Gardiner, C.L. Raston, Coord. Chem. Rev. 166 (1997) 1.

[9] M.A. Khan, D.T. Olson, J.N. Kuznia, Appl. Phys. Lett. 65 (1994) 64.

[10] M.G. Simmonds, W.L. Gladfelter, in: T. Kodas, M. Hampden-Smith (Eds.), Chemical Vapor Deposition of Aluminum, VCH, Weinheim, 1994.

[11] K. Tsubouchi, K. Masu, Vacuum 46 (1995) 1249.

[12] T. Wadayama, Y. Maiwa, H. Shibata, A. Hatta, Jpn. J. Appl. Phys. 34 (1995) L779.

[13] H. Sakaue, Y. Katsuda, S. Konagata, S. Shingubara, Jpn. J. Appl. Phys. 35 (1996) 1010.

[14] J.-H. Yun, J.-H. Lee, J.W. Park, S.-W. Rhee, J. Electrochem. Soc. 145 (1998) L23.

[15] T. Amazawa, J. Electrochem. Soc. 145 (1998) 4327.

[16] J.-H. Lee, M.-Y. Park, J.-H. Yun, S.-W. Rhee, Thin Solid Films 348 (1999) 130.

[17] T.-C. Shen, C. Wang, J.R. Tucker, Appl. Surf. Sci. 141 (1999) 228.

[18] E. Kondoh, T. Ohta, J. Vac. Sci. Technol. A 13 (1995) 2863.

[19] M. Naik, T. Guo, L. Chen, R. Mosely, I. Beinglass, J. Vac. Sci. Technol. A 16 (1998) 1233.

[20] T. Mitsui, E. Hill, R. Curtis, E. Ganz, Phys. Rev. B 59 (1999) 8123.

[21] K.A. Littau, R. Mosely, S. Zhou, H. Zhang, T. Gou, Microelectronic Eng. 33 (1997) 101.

[22] Y. Matsumiya, K. Nakajima, J. Cryst. Growth 181 (1997) 437.

[23] M. Okawa, H. Tsuruta, M. Hanabusa, Appl. Surf. Sci. 79/80 (1994) 444.

[24] T. Kawai, M. Okawa, A. Komatsu, T. Shimada, M. Hanabusa, Appl. Surf. Sci. 79/80 (1994) 385.

[25] T. Wadayama, Y. Maiwa, H. Shibata, A. Hatta, Appl. Surf. Sci. 100/101 (1996) 575.

[26] M. Hanabusa, T. Nitta, Appl. Surf. Sci. 106 (1996).

[27] X. Li, B.-Y. Kim, S.-W. Rhee, Appl. Phys. Lett. 67 (1995) 3246.

[28] D.M. Frigo, F.J.M. van Eijden, P.J. Reuvers, C.J. Smit, Chem. Mater. 6 (1994) 190.

[29] M.G. Simmonds, W.L. Gladfelter, H. Li, P.H. McMurry, J. Vac. Sci. Technol. A 11 (1993) 3026.

[30] M.G. Simmonds, I. Taupin, W.L. Gladfelter, Chem. Mater. 6 (1994) 935.

[31] N. Venkateswaren, I. Karpov, W. Gladfelter, A. Franciosi, J. Vac. Sci. Technol. A 14 (1996) 1949.

[32] T.W. Jang, W. Moon, J.T. Baek, B.T. Ahn, Thin Solid Films 333 (1998) 137.

[33] T.W. Jang, H.S. Rhee, B.T. Ahn, J. Vac. Sci. Technol. A 13 (1999) 1031.

[34] J. Han, K.F. Jensen, Y. Senzaki, W.L. Gladfelter, Appl. Phys. Lett. 64 (1994) 425.

[35] B.-Y. Kim, X. Li, S.-W. Rhee, Appl. Phys. Lett. 68 (1996) 3567.

[36] I. Karpov, W. Gladfelter, A. Franciosi, Appl. Phys. Lett. 69 (1996) 4191.

[37] Y. Neo, T. Otoda, K. Sagae, H. Mimura, K. Yokoo, Jpn. J. Appl. Phys. 37 (1998) 2602.

[38] I. Karpov, G. Bratina, L. Sorba, A. Franciosi, M.G. Simmonds, W.L. Gladfelter, J. Appl. Phys. 76 (1994) 3471.

[39] C. Popov, B. Ivanov, V. Shanov, J. Appl. Phys. 75 (1994) 3687.

[40] J.-H. Yun, B.-Y. Kim, S.-W. Rhee, Thin Solid Films 312 (1998) 259.

[41] K. Hayama, T. Togun, M. Ishida, J. Cryst. Growth 179 (1997) 438.

[42] Y. Neo, M. Niwano, H. Mimura, K. Yokoo, Appl. Surf. Sci. 142 (1999) 443.

[43] D. Tonneau, F. Thuron, A. Correia, J.E. Bouree, Y. Pauleau, Jpn. J. Appl. Phys. 38 (1998) 4954.

[44] J.J.A. Glass, S.-D. Hwang, S. Data, B. Robertson, J.T. Spencer, J. Phys. Chem. Solids 57 (1996) 563.

[45] F.M. Elms, R.N. Lamb, P.J. Pigram, M.G. Gardiner, B.J. Wood, C.L. Raston, Chem. Mater. 6 (1994) 1059.

[46] A.T.S. Wee, A.J. Murrell, N.K.; Singh, D. O'Hare, J.S. Foord, J. Chem. Soc. Chem. Commun. 1990, 11.

[47] L.H. Dubois, B.R. Zegarski, M.E. Gross, R.G. Nuzzo, Surf. Sci. 244 (1991) 89.

[48] D.-H. Kim, M.-Y. Park, S.-W. Rhee, Journal of Materials Science–Materials in Electronics (1999) 285.

[49] H. Choi, S. Hwang, Chem. Mater. 10 (1998) 2323.

[50] A.C. Jones, D.J. Houlton, S.A. Rushworth, J.A. Flanagan, J.R. Brown, G.W. Critchlow, Chem. Vap. Deposition 1 (1995) 24.

[51] I. Karpov, A. Franciosi, C. Taylor, J. Roberts, W.L. Gladfelter, Appl. Phys. Lett. 71 (1997) 3090.

[52] J.A. Haber, W.E. Buhro, J. Am. Chem. Soc. 120 (1998) 10847.

[53] C.E. Johnson, K.T. Higa, Mater. Res. Soc. Symp. Proc. 457 (1997) 131.

[54] S.T. Schwab, P.P. Paul, Y.-M. Pan, Mater. Sci. Eng. A 204 (1995) 197.

[55] J.A. Haber, J.L. Crane, W.E. Buhro, C.A. Frey, S.M.L. Sastry, J.J. Balbach, M.S. Conradi, Adv. Mater. 8 (1996) 163.

[56] T.F. Kuech, D.J. Wolford, E. Veuhoff, V. Deline, P.M. Mooney, R. Potenski, J. Bradley, J. Appl. Phys. 62 (1987) 632.

[57] V. Frese, G.K. Regel, H. Hardtdegen, A. Brauners, P. Balk, M. Hostalek, M. Lokai, L. Pohl, A. Miklis, K. Werner, J. Electron. Mater. 19 (1990) 305.

[58] R. Jothilingam, T. Farrell, T.B. Joyce, P.J. Goodhew, J. Cryst. Growth 188 (1998) 39.

[59] K. Miyakoshi, I. Suemune, Appl. Phys. Lett. 64 (1994) 1549.

[60] C.R. Abernathy, S.J. Pearton, F.A. Baiocchi, T. Ambrose, A.S. Jordan, D.A. Bohling, G.T. Muhr, J. Cryst. Growth 110 (1991) 457.

[61] C.R. Abernathy, P.W. Wisk, Solid-State Electronics 38 (1995) 737.

[62] N.G. Paraskevopoulos, S.R. McAfee, W.S. Hobson, Appl. Phys. Lett. 66 (1995) 183.

[63] M. Nagano, S. Iwai, K. Nemoto, Y. Aoyagi, Jpn. J. Appl. Phys. 33 (1994) L1289.

[64] M. Miyashita, H. Kizuki, M. Tsugami, N. Fujii, Y. Mihashi, S. Takamiya, J. Cryst. Growth 192 (1998) 79.

[65] S. Hirose, N. Kano, K. Hara, H. Nunekata, H. Kukimoto, J. Cryst. Growth 172 (1997) 13.

[66] B. Courboules, C. Deparis, J. Massies, M. Leroux, C. Grattepain, Appl. Phys. Lett. 65 (1994) 836.

[67] P.R. Hageman, S.M. Olsthoorn, L.J. Giling, J. Cryst. Growth 142 (1994) 284.

[68] R.W. Freer, T. Martin, P.A. Lane, C.R. Whitehouse, T.J. Whitaker, M. Houlton, P.D.J. Calcott, D. Lee, A.C. Jones, S.A. Rushworth, J. Cryst. Growth 150 (1995) 539.

[69] S. Hirose, M. Yamaura, A. Yoshida, H. Ibuka, K. Hara, H. Munekata, J. Cryst. Growth 194 (1998) 16.

[70] N. Kano, S. Hirose, K. Hara, J. Yoshino, H. Munekata, H. Kukimoto, Appl. Surf. Sci. 82/83 (1994) 132.

[71] H.Q. Hou, W.G. Brieland, B.E. Hammons, R.M. Biefeld, K.C. Baucom, R.A. Stall, J. Electronic Mater. 26 (1997) 1178.

[72] S. Yoshida, M. Sasaki, J. Cryst. Growth 156 (1995).

[73] S. Yoshida, M. Sasaki, J. Cryst. Growth 164 (1996) 291.

[74] R. Bhat, M.A. Koza, C.C. Chang, S.A. Schwarz, T.D. Harris, J. Cryst. Growth 77 (1986) 7.

[75] S. Yoshida, M. Sasaki, J. Cryst. Growth 152 (1995) 347.

[76] R. Hovel, E. Steimetz, K. Heime, J. Cryst. Growth 145 (1994) 498.

[77] R.M. Biefeld, A.A. Allerman, M.W. Pelczynski, Appl. Phys. Lett. 68 (1996) 932.

[78] R.M. Biefeld, S.R. Kurtz, A.A. Allerman, J. Electron. Mater. 26 (1997) 903.

[79] R. Tsui, K. Shiralagi, J. Shen, J. Cryst. Growth 164 (1996) 491.

[80] G.J. Bauhuis, P.R. Hageman, P.K. Larsen, J. Cryst. Growth 191 (1998) 313.

[81] Y. Takahashi, K. Yamashita, S. Motojima, K. Sugiyama, Surf. Sci. 86 (1979) 238.

[82] D.C. Bertolet, H. Liu, J.W. Rogers, J. Appl. Phys. 75 (1994) 5383.

[83] M.A. Khan, Q. Chen, C.J. Sun, M. Shur, B. Gelmont, Appl. Phys. Lett. 67 (1995) 1429.

[84] H. Liu, J.W. Rogers, J. Vac. Sci. Technol. A 17 (1999) 325.

[85] P.R. Chalker, T.B. Joyce, T. Farrell, Diamond Related Mater. 8 (1999) 373.

[86] J.N. Kidder, J.S. Kuo, A. Ludviksson, T.P. Pearsall, J.W. Rogers, J.M. Grant, L.R. Allen, S.-T. Hsu, J. Vac. Sci. Technol. A 13 (1995) 711.

[87] J.N. Kidder, H.K. Yun, J.W. Rogers, T.P. Pearsall, Chem. Mater. 10 (1998) 777.

[88] A. Ludviksson, D.W. Robinson, J.W. Rogers, Thin Solid Films 289 (1996) 6.

[89] J.D. Mackenzie, C.R. Abernathy, J.D. Stewart, G.T. Muhr, J. Cryst. Growth 164 (1996) 143.

[90] C.L. Aardahl, J.W. Rogers, H.K. Yun, Y. Ono, D.J. Tweet, S.-T. Hsu, Thin Solid Films 346 (1999) 174.

[91] J.S. Foord, T.J. Whitaker, D. O'Hare, A.C. Jones, J. Cryst. Growth 136 (1994) 127.

[92] J. McMurran, J. Kouvetakis, D. Smith, J. Appl. Phys. Lett. 74 (1999) 883.

[93] J. McMurran, J. Kouvetakis, D.C. Nesting, D.J. Smith, J.L. Hubbard, J. Am. Chem. Soc. 120 (1998) 5233.

[94] J. McMurran, D. Dai, K. Balasubramanian, C. Steffek, J. Kouvetakis, J.L. Hubbard, Inorg. Chem. 37 (1998) 6638.

[95] R.L. Wells, W.L. Gladfelter, J. Cluster Sci. 8 (1997) 217.

[96] J.F. Janik, R.T. Paine, J. Organomet. Chem. 449 (1993) 39.

[97] J.A. Haber, P.C. Gibbons, W.E. Buhro, J. Am. Chem. Soc. 119 (1997) 5455.

[98] D. Dou, D.R. Ketchum, E.J.M. Hamilton, P.A. Florian, K.E. Vermillion, P.J. Grandinetti, S.G. Shore, Chem. Mater. 8 (1996) 2839.

[99] J.-W. Hwang, S.A. Hanson, D. Britton, J.F. Evans, K.F. Jensen, W.L. Gladfelter, Chem. Mater. 2 (1990) 342.

[100] J.-W. Hwang, J.P. Campbell, J. Kozubowski, S.A. Hanson, J.F. Evans, W.L. Gladfelter, Chem. Mater. 7 (1995) 517.

[101] J.P. Campbell, J.-W. Hwang, R.B. Von Dreele, C.J. Cramer, W.L. Gladfelter, J. Am. Chem. Soc. 120 (1998) 521.

[102] J.L. Coffer, M.A. Johnson, L. Zhang, R.L. Wells, J.F. Janik, Chem. Mater. 9 (1997) 2671.

[103] J.F. Janik, R.L. Wells, Inorg. Chem. 36 (1997) 4135.

[104] J.A. Jegier, S. McKernan, W.L. Gladfelter, Chem. Mater. 10 (1998) 181.

[105] J.A. Jegier, S. McKernan, W.L. Gladfelter, Inorg. Chem. 38 (1999) 2726.

[106] J.A. Jegier, S. McKernan, A.P. Purdy, W.L. Gladfelter, Chem. Mater. (in press).

[107] J.F. Janik, R.L. Wells, V.G. Young Jr., A.L. Rheingold, I.A. Guzei, J. Am. Chem. Soc. 120 (1998) 532.

[108] K. Hayama, T. Togun, M. Ishida, J. Cryst. Growth 179 (1997) 433.

[109] J.F. Moore, D.R. Strongin, P.B. Comita, M.W. Ruckman, M. Strongin, Appl. Phys. Lett. 65 (1994) 368.

[110] R.J. Wehmschulte, P.P. Power, J. Am. Chem. Soc. 119 (1997) 9566.